Peculiar Rashba Splitting Originating from the Two-Dimensional Symmetry of the Surface

Kazuyuki Sakamoto,[1,*] Haruya Kakuta,[1] Katsuaki Sugawara,[2] Koji Miyamoto,[3] Akio Kimura,[4] Takuya Kuzumaki,[1] Nobuo Ueno,[1] Emilia Annese,[5] Jun Fujii,[5] Ayaka Kodama,[6] Tatsuya Shishidou,[6] Hirofumi Namatame,[3] Masaki Taniguchi,[4] Takafumi Sato,[7] Takashi Takahashi,[2,7] and Tamio Oguchi[6]

[1]*Graduate School of Advanced Integration Science, Chiba University, Chiba 263-8522, Japan*
[2]*WPI Research Center, Advanced Institute for Materials Research, Tohoku University, Sendai 980-8577, Japan*
[3]*Hiroshima Synchrotron Radiation Center, Hiroshima University, Higashi-Hiroshima 739-0046, Japan*
[4]*Graduate School of Science, Hiroshima University, Higashi-Hiroshima 739-8526, Japan*
[5]*TASC National Laboratory, INFM-CNR, SS 14, km 163.5, I-34012 Trieste, Italy*
[6]*Department of Quantum Matter, ADSM, Hiroshima University, Higashi-Hiroshima 739-8530, Japan*
[7]*Department of Physics, Tohoku University, Sendai 980-8578, Japan*

(Received 20 July 2009; published 5 October 2009)

A peculiar Rashba effect is found at a point in the Brillouin zone, where the time-reversal symmetry is broken, though this symmetry was believed to be a necessary condition for Rashba splitting. This finding obtained experimentally by photoemission measurements on a Bi/Si(111)-($\sqrt{3} \times \sqrt{3}$) surface is fully confirmed by a first-principles theoretical calculation. We found that the peculiar Rashba effect is simply understood by the two-dimensional symmetry of the surface, and that this effect leads to an unconventional nonvortical Rashba spin structure at a point with time-reversal invariance.

DOI: 10.1103/PhysRevLett.103.156801 PACS numbers: 73.20.−r, 71.70.−d, 73.20.At

The so-called Rashba-Bychkov (RB) (or simply Rashba) effect [1] is a novel low-dimensional physical property that produces a spin-polarized two-dimensional (2D) electron gas even for nonmagnetic materials, and is the key concept of many promising proposed spintronic devices [2–6]. In a structural inversion asymmetric environment such as a crystal surface, the spin degeneracy is lifted by the spin-orbit interaction that leads to a pair of split bands in the momentum ($\vec{k}$) space. The split band is a completely polarized electronic state with the spin polarization vector ($\vec{P}$) in the surface plane, the directions of the $\vec{P}$ of the two bands are opposite, and the constant energy contour shows a vortical spin structure in an ideal 2D system [Figs. 1(a) and 1(b)]. This spin-splitting effect has been observed on clean noble metal surfaces [7–12] and heavy group V elements [13–15], and has recently been reported to be enhanced in systems in which heavy element atoms are adsorbed on light element substrates [16–18]. The spin-split bands observed in these studies show similar behavior as that of the simple RB effect; i.e., they show pairs of split bands in the $\vec{k}$ space around the $\bar{\Gamma}$ point and the $\vec{P}$ almost lies in the surface plane. The simple RB splitting is considered to arise at wave vectors with time-reversal symmetry [$E(\vec{q} + \vec{k}, \vec{P}) = E(\vec{q} - \vec{k}, -\vec{P})$], and thus the split has the possibility to occur at symmetry points of the surface Brillouin zone (SBZ) boundary in addition to $\bar{\Gamma}$, i.e., at $\vec{q} = 0$ and $\vec{G}/2$ where $\vec{G}$ is the reciprocal lattice vector. However, as opposed to the simple RB effect, a curious spin splitting has been reported to occur at a particular symmetry point, the $\bar{K}$ point with a C_3 symmetry of a Si(111)-(1 × 1) surface formed by the adsorption of one monolayer (ML) of Tl [19]. This implies that the symmetry of the surface, which was not considered earnestly so far, can affect the RB spin, and therefore that a proper understanding of the RB effect on surfaces with different symmetry is indispensable [19,20].

In this Letter, we report the RB effect of the β-Bi/Si(111)-($\sqrt{3} \times \sqrt{3}$) surface (hereafter the β-Bi surface) that belongs to the plane group $p31m$, a group that is different from that of the Tl/Si(111) surface, $p3m1$. This β-Bi surface is formed by the adsorption of 1 ML of Bi on Si(111) that leads to a ($\sqrt{3} \times \sqrt{3}$) structure with Bi trimers as shown in Fig. 1(c) [21–23]. The difference in plane group leads to a $\bar{K}$ point with C_{3v} symmetry on β-Bi, a symmetry different from that on Tl/Si(111). We found that although the time-reversal symmetry was regarded as a

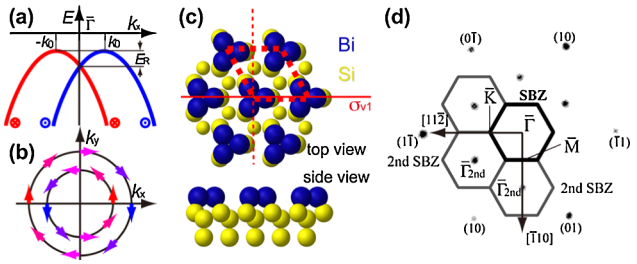

FIG. 1 (color online). (a) Dispersion of a spin-split surface state band resulting from the RB effect. k_0 is the offset by which the $E(\vec{k}_x)$ parabola is shifted away from the $\bar{\Gamma}$ point, and E_R is the Rashba energy of the split bands. (b) Constant energy contour of the split bands. (c) Schematic illustrations of the β-Bi/Si(111)-($\sqrt{3} \times \sqrt{3}$) surface. The thick dashed lines indicate the unit cell of this surface. (d) SBZs and LEED pattern of the surface. $\bar{\Gamma}$, $\bar{M}$, and $\bar{K}$ are the symmetry points of the ($\sqrt{3} \times \sqrt{3}$) SBZ.

 © 2009 The American Physical Society

necessary condition for RB splitting and $\bar{K}$ does not have such symmetry ($\vec{q} \neq \vec{G}/2$ and thus $E(\vec{q}+\vec{k},\vec{P}) \neq E(\vec{q}-\vec{k},-\vec{P})$ at $\bar{K}$), a $\bar{K}$ point with C_{3v} symmetry shows a peculiar RB splitting, i.e., a RB splitting without time-reversal invariance. Further, the peculiar vortical RB splitting at $\bar{K}$ and the normal vortical spin structure at $\bar{\Gamma}$ lead to a specific nonvortical RB splitting at the $\bar{M}$ point, a point with time-reversal invariance. (A nonvortical RB spin structure is not expected in the case of a normal RB effect with time-reversal invariance.) These novel quantum phenomena, which imply that the time-reversal symmetry is not a necessary and sufficient condition for a RB effect, are corroborated by the combination of high-resolution angle-resolved photoelectron spectroscopy (ARPES) and spin-resolved (SR)-ARPES measurements, and a state-of-the-art theoretical calculation.

The high-resolution ARPES measurements were performed with a VG-SCIENTA SES-2002 analyzer by using an unpolarized He Iα radiation light ($h\nu = 21.218$ eV) at Tohoku University, and a linearly polarized synchrotron radiation light ($h\nu = 20$–25 eV) at the low energy branch of the APE-INFM beam line [24] at Elettra, Trieste, Italy. The SR-ARPES measurements have been performed in a spin-resolved photoemission system of the Hiroshima Synchrotron Radiation Center, Hiroshima University, Japan. The energy and angular resolutions were 10–25 meV and 0.2° in the ARPES measurements, and 200 meV and 2° in the SR-ARPES one. Bi was deposited on a Si(111)-(7×7) clean surface, which was obtained by annealing at 1520 K, from a Knudsen cell at a substrate temperature of 570 K. The base pressure was below 5×10^{-11} Torr during the measurements, and below 5×10^{-10} Torr during the Bi evaporation. The theoretical calculations are based on the first-principles density-functional approach, in which one electron Kohn-Sham equations are solved with the all-electron full-potential linear augmented-plane-wave method including the spin-orbit coupling as a second variation in self-consistent-field iterations. A 12-layer slab, which one side is terminated by 1 ML of Bi atoms and the other is saturated by hydrogen atoms, was used. In addition, a 24-layer slab was also adopted to check the thickness effects on the surface relaxation and electronic structure.

Figure 1(d) shows the low-energy electron diffraction (LEED) pattern of the β-Bi surface together with the SBZs of the sample. The LEED spots are shown by black spots. As shown in the figure, the intensities of the (10), $(\bar{1}1)$ and $(0\bar{1})$ spots are the same, but those of the (01), $(\bar{1}0)$ and $(1\bar{1})$ spots are stronger. This inequivalency results from the threefold symmetry of the system, which is obvious by looking at the atomic structure shown in Fig. 1(c). The threefold symmetry and the presence of mirror planes along the $[11\bar{2}]$ direction and its two other equivalent directions lead to a C_{3v} symmetry for the $\bar{\Gamma}$ and $\bar{K}$ points, and a C_{1h} symmetry for the $\bar{M}$ point. Of the three symmetry points, $\bar{\Gamma}$ and $\bar{M}$ of the $(\sqrt{3}\times\sqrt{3})$ surface have the same symmetry as those of a (1×1) surface [19], while the symmetry of $\bar{K}$ is different on the two surfaces. The different symmetry at $\bar{K}$ results from the difference in symmetry of the $\bar{\Gamma}$-$\bar{K}$ direction; i.e., $\bar{\Gamma}$-$\bar{K}$ is along the $[11\bar{2}]$ direction that has a mirror symmetry on a $(\sqrt{3}\times\sqrt{3})$ surface while it is along the $[\bar{1}10]$ direction that has no mirror symmetry on a (1×1) surface.

The electronic band dispersion of β-Bi measured along the $\bar{\Gamma}$-$\bar{M}$-$\bar{\Gamma}$ direction is displayed in Fig. 2(a). The two bands denoted as B originate from the electronic state of bulk Si. Besides these B states, three states are observed at binding energies (E_B's) of 0.53 eV, 0.91 eV, and 1.35 eV at the $\bar{M}$ point, and three states at 1.25 eV, 1.45 eV, and 1.83 eV at the $\bar{\Gamma}$ point of the second SBZ. All of these three states follow a $(\sqrt{3}\times\sqrt{3})$ periodicity, and indicate that β-Bi has at least three surface states (or surface resonance states). This agrees well with the number reported in the literature [18,25,26], though the dispersion behaviors reported in Refs. [25,26] are different from the present ones, and the E_B's of the surface states in Ref. [18] are ca. 0.6 eV higher than those shown in Fig. 2. The difference in dispersion behaviors might result from the higher energy and angular resolutions of the system and/or the higher sample quality used in the present study, and the difference in E_B's would result from the different surface photovoltage (SPV) shifts [27]. A different SPV shift is obtained when the sample is annealed at a different temperature during the cleaning procedure, and the observed difference in E_B's is well explained by the difference in SPV shifts expected by the temperatures used in the two studies.

As displayed in Fig. 2(a), all the three surface states show RB-type splitting along the $\bar{\Gamma}$-$\bar{M}$-$\bar{\Gamma}$ direction ($S1$ and $S2$ show clear splits at $\bar{M}$, and the split of $S3$ is clearly

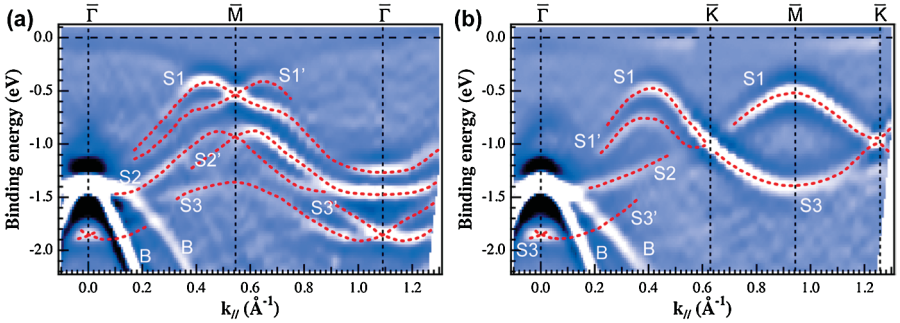

FIG. 2 (color). Band structures measured along the (a) $\bar{\Gamma}$-$\bar{M}$-$\bar{\Gamma}$ and (b) $\bar{\Gamma}$-$\bar{K}$-$\bar{M}$ directions. The horizontal dashed line at $E_B = 0$ eV indicates the Fermi level. The red-dashed lines are the band structures obtained by tracing the peak and shoulder structures in the photoemission spectra.

observed at $\bar{\Gamma}$). By characterizing the splits using the Rashba energy E_R and the momentum offset k_0 [Fig. 1(a)], we obtain $E_R = 120$ meV and $k_0 = 0.105$ Å^{-1} for $S1$, $E_R = 60$ meV and $k_0 = 0.07$ Å^{-1} for $S2$, and $E_R = 60$ meV and $k_0 = 0.08$ Å^{-1} for $S3$. Of the three surface state bands, the split of $S2$ and $S3$ have not been observed so far. Regarding the $S1$ state, a similar split has been observed in Refs. [18,25], but not in Ref. [26]. These mean that the RB-type splitting of the three surface bands are not yet understood properly.

The three surface states are observed along the $\bar{\Gamma}$-$\bar{K}$-$\bar{M}$ direction as well [Fig. 2(b)]. The $S1$ and $S3$ bands show splits in the $k_{\|}$ range from $\bar{\Gamma}$ to $\bar{K}$, but no clear split was observed for $S2$. Regarding the $k_{\|}$ range from $\bar{K}$ to $\bar{M}$, only the $S1$ and $S3$ bands that do not show clear splits in this range are observable. ($S1$ and $S3$ are assigned by their E_B's at $\bar{M}$.) Here we note that the energy widths of both $S1$ and $S3$ obtained in this $k_{\|}$ range were ca. 1.5 times larger than the widths of $S1$ and $S3$ obtained around the $\bar{M}$ and $\bar{\Gamma}$ points of Fig. 2(a). This difference in width indicates that the "single" $S1$ band and the "single " $S3$ band observed from $\bar{K}$ to $\bar{M}$ in Fig. 2(b) would consist of split bands that are not resolved due to the limited experimental resolution.

In Figs. 3(a) and 3(b), we show the calculated band structure along (a) the $\bar{\Gamma}$-$\bar{M}$-$\bar{\Gamma}$ direction and (b) the $\bar{\Gamma}$-$\bar{K}$-$\bar{M}$ direction together with the ARPES results. The black dots and colored filled circles are the calculated bands (the two colors indicate the opposite two $\vec{P}$'s). The size of the red and blue filled circles represents the degree of spin polarization whose direction corresponds to the $\vec{P}$ of a normal RB spin [Fig. 3(i)] with the p-orbital components of Bi. As shown in Figs. 3(a) and 3(b), the calculation reproduces well the three surface states along both directions [28,29]. Of the three states, the calculated split bands of $S1$ ($S1$ and $S1'$) show clear opposite spin polarization around the $\bar{M}$ and $\bar{K}$ points, and those of $S3$ ($S3$ and $S3'$) show an opposite spin polarization around $\bar{\Gamma}$. These results agree well with the spin polarization observed in the SR-ARPES spectra shown in Figs. 3(c)–3(e). Taking the direction of $\vec{P}$ into account, we conclude that the splits of the these surface bands observed along the $\bar{\Gamma}$-$\bar{M}$-$\bar{\Gamma}$ direction originate from RB effects, whose Rashba parameters ($\alpha_R \sim 2E_R/k_0$) are ~2.3 eV Å for $S1$ and ~1.5 eV Å for $S3$. (The α_R of $S1$ agrees well with the value reported recently [18].)

Since there is no time-reversal symmetry around $\bar{K}$, this point has not been considered to show a RB splitting so far. In order to understand the origin of the split of $S1$ observed around $\bar{K}$, we discuss the symmetry at this point on the basis of group theory. The symmetry at $\bar{K}$ is C_{3v}, the same symmetry as that at $\bar{\Gamma}$ on the β-Bi surface. The 2D irreducible representation of the C_{3v} group reveals the isotropic spin splitting and vortical spin structure that is given by the RB Hamiltonian, $H_{\mathrm{RB}} = \alpha_R(|\epsilon|)\vec{\sigma} \cdot (\vec{k}_{\|} \times \hat{e}_z)$, regardless of the existence of time-reversal symmetry [20]. This means that the split observed around $\bar{K}$ would be a RB-type spin splitting, but which is referred to as a peculiar RB splitting in the sense that it cannot be given by the time-

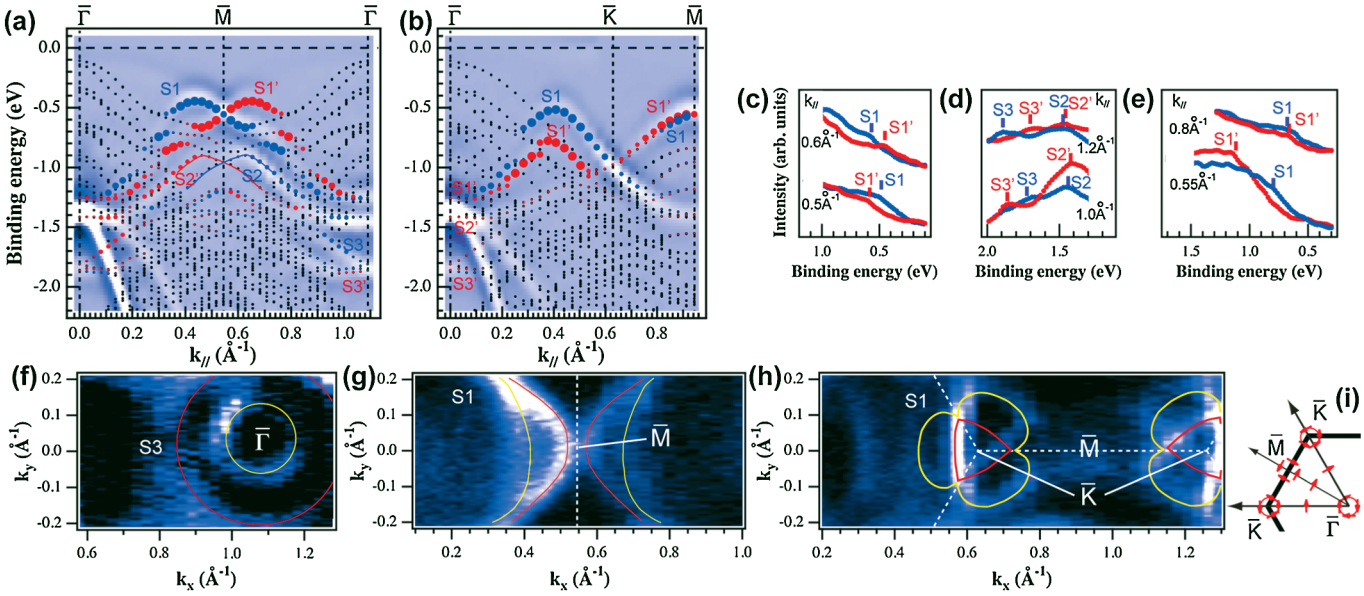

FIG. 3 (color). Calculated band dispersions along the (a) $\bar{\Gamma}$-$\bar{M}$-$\bar{\Gamma}$ direction and (b) $\bar{\Gamma}$-$\bar{K}$-$\bar{M}$ direction together with the experimental results. Black dots are the calculated bands, and the red and blue filled circles are the calculated spin-polarized electronic states. (c) and (d) are the SR-ARPES spectra measured along the $\bar{\Gamma}$-$\bar{M}$-$\bar{\Gamma}$ direction, and (e) shows the spectra along $\bar{\Gamma}$-$\bar{K}$-$\bar{M}$. The directions of $\vec{P}$'s are the same as those of normal RB spins in (c)–(e). (f)–(h) display the constant energy contours around the $\bar{\Gamma}$ point of the second SBZ at $E_B = 1.7$ eV, around $\bar{M}$ at $E_B = 0.45$ eV, and along the $\bar{K}$-$\bar{M}$-$\bar{K}$ direction at $E_B = 0.85$ eV. The dashed lines in (g) and (h) are the SBZ boundaries. (i) A schematic illustration of the RB spin on a β-Bi surface. The arrows show the $\vec{P}$ of one of the split bands, as derived from the normal RB effect.

reversal symmetry that was believed to be a necessary condition for RB splitting, but by the consequence of the group symmetry.

In order to discuss the RB splitting at the three symmetry points in more detail, we have measured the constant energy contours of $S3$ around the $\bar{\Gamma}$ point, and those of $S1$ around $\bar{M}$ and $\bar{K}$. Figures 3(f)–3(h) are the constant energy contours around the $\bar{\Gamma}$ point of the second SBZ at $E_B = 1.7$ eV, around $\bar{M}$ at $E_B = 0.45$ eV, and along the $\bar{K}$-$\bar{M}$-$\bar{K}$ direction at $E_B = 0.85$ eV. k_x corresponds to the $\bar{\Gamma}$-$\bar{M}$-$\bar{\Gamma}$ direction in (f) and (g), and to the $\bar{\Gamma}$-$\bar{K}$-$\bar{M}$ direction in (h). The dashed lines in (g) and (h) are the SBZ boundaries. The two round circles observed in Fig. 3(f) indicate the presence of isotropic spin splitting and vortical spin structure of $S3$ around the $\bar{\Gamma}$ point, and therefore that the split observed around this symmetry point results from a simple RB effect such as the schematic illustration in Fig. 1(b). In contrast to this ''ideal'' case, Figs. 3(g) and 3(h) show peculiar constant energy contours. That is, the curves in Fig. 3(g) are not closed, and the curves in Fig. 3(h) are quite distorted (the peculiar shapes of these constant energy contours have been confirmed by the theoretical calculation). However, despite of their distorted shapes, the closed structure in Fig. 3(h) indicates that $S1$ shows a vortical spin structure around the $\bar{K}$ point. (The distorted shapes would originate from the crystal field that is generally stronger at the boundary of the SBZ.) Taking the vortical spin structure around $\bar{K}$ and the C_{3v} symmetry of this point into account, we conclude that the split of $S1$ observed around the $\bar{K}$ point definitely results from a peculiar RB effect which is given without a time-reversal symmetry.

The vortical spin structures around the $\bar{K}$ and $\bar{\Gamma}$ points lead to a nonvortical spin structure at the $\bar{M}$ point as shown in the schematic illustration in Fig. 3(i). The arrows in Fig. 3(i) show the $\vec{P}$ of one of the split bands, as derived from the normal RB effect. This nonvortical spin structure, which is observed as unclosed curves in the constant energy contour shown in Fig. 3(g), indicates the presence of a peculiar RB splitting at the $\bar{M}$ point that has not been observed on any other system so far, and therefore demonstrates that the time-reversal symmetry is not a sufficient condition to obtain a normal RB splitting with vortical spin structure.

In conclusion, our study reveals that a 2D system with threefold symmetry, in which the $\bar{K}$ point has a C_{3v} symmetry, exhibits peculiar RB splitting at both the $\bar{K}$ and $\bar{M}$ points. The peculiar RB effect at $\bar{K}$, which shows a distorted vortical spin structure, is given by not a time-reversal symmetry that was believed to be a necessary condition for RB splitting, but by the 2D symmetry of this point. This distorted vortical structure affects the RB effect at $\bar{M}$, which has a time-reversal invariance and thus has been considered to show a normal RB splitting. That is, it guides the RB splitting to a specific nonvortical spin structure around the $\bar{M}$ point. These results imply that the time-reversal symmetry is not a necessary and sufficient condition for a RB effect, and that knowledge on the 2D symmetry of the system is indispensable for understanding the RB effect properly.

Experimental supports from Y. Tago, K. Kuroda, and K. Kanomaru are gratefully acknowledged. This work was financially supported by the JSPS Grant-in-Aid for Scientific Research (A) 20244045 and (B) 20340092, and the G-COE program of MEXT (G-03).

*kazuyuki_sakamoto@faculty.chiba-u.jp

[1] Y. A. Bychkov and E. I. Rashba, JETP Lett. **39**, 78 (1984).
[2] S. Datta and B. Das, Appl. Phys. Lett. **56**, 665 (1990).
[3] J. Nitta, T. Akazaki, H. Takayanagi, and T. Enoki, Phys. Rev. Lett. **78**, 1335 (1997).
[4] Y. Kato, R. C. Myers, A. C. Gossard, and D. D. Awschalom, Nature (London) **427**, 50 (2004).
[5] J. Sinova *et al.*, Phys. Rev. Lett. **92**, 126603 (2004).
[6] D. D. Awschalom and M. E. Flatté, Nature Phys. **3**, 153 (2007).
[7] S. LaShell, B. A. McDougall, and E. Jensen, Phys. Rev. Lett. **77**, 3419 (1996).
[8] G. Nicolay, F. Reinert, S. Hüfner, and P. Blaha, Phys. Rev. B **65**, 033407 (2001).
[9] M. Hoesch *et al.*, Phys. Rev. B **69**, 241401(R) (2004).
[10] D. Popovic *et al.*, Phys. Rev. B **72**, 045419 (2005).
[11] H. Cercellier *et al.*, Phys. Rev. B **73**, 195413 (2006).
[12] D. Malterre *et al.*, New J. Phys. **9**, 391 (2007).
[13] Yu. M. Koroteev *et al.*, Phys. Rev. Lett. **93**, 046403 (2004).
[14] K. Sugawara *et al.*, Phys. Rev. Lett. **96**, 046411 (2006).
[15] T. Hirahara *et al.*, Phys. Rev. Lett. **97**, 146803 (2006).
[16] C. R. Ast *et al.*, Phys. Rev. Lett. **98**, 186807 (2007).
[17] F. Meier *et al.*, Phys. Rev. B **77**, 165431 (2008).
[18] I. Gierz *et al.*, Phys. Rev. Lett. **103**, 046803 (2009).
[19] K. Sakamoto *et al.*, Phys. Rev. Lett. **102**, 096805 (2009).
[20] T. Oguchi and T. Shishidou, J. Phys. Condens. Matter **21**, 092001 (2009).
[21] T. Takahashi *et al.*, Surf. Sci. **191**, L825 (1987); S. Nakatani *et al.*, Phys. Rev. B **52**, R8711 (1995).
[22] R. H. Miwa, T. M. Schmidt, and G. P. Srivastava, J. Phys. Condens. Matter **15**, 2441 (2003).
[23] K. J. Wan, T. Guo, W. K. Ford, and J. C. Hermanson, Phys. Rev. B **44**, 3471 (1991).
[24] G. Panaccione *et al.*, Rev. Sci. Instrum. **80**, 043105 (2009).
[25] T. Kinoshita, S. Kono, and H. Nagayoshi, J. Phys. Soc. Jpn. **56**, 2511 (1987).
[26] Y. Kim *et al.*, J. Korean Phys. Soc. **39**, 1032 (2001).
[27] H. M. Zhang, K. Sakamoto, G. V. Hansson, and R. I. G. Uhrberg, Phys. Rev. B **78**, 035318 (2008).
[28] In order to obtain the best correspondence with the experimental data, the energy scale of the calculated band structure is magnified by ca. 5%.
[29] The calculated bands observed in the E_B range from 0.1 to 0.7 eV at $\bar{\Gamma}$, are not observed experimentally due to the high surface sensitivity of the photon energy used in the present study.